Pre-Steady-State Studies of Phosphite Dehydrogenase Demonstrate That Hydride Transfer Is Fully Rate Limiting†

Emily J. Fogle and Wilfred A. van der Donk*

Department of Chemistry, University of Illinois at Urbana-Champaign, 600 South Mathews Avenue, Urbana, Illinois 61801

Received August 2, 2007; Revised Manuscript Received September 3, 2007

ABSTRACT: Phosphite dehydrogenase (PTDH) is a unique NAD-dependent enzyme that catalyzes the oxidation of inorganic phosphite to phosphate. The enzyme has great potential for cofactor regeneration, and mechanistic studies have provided some insight into the residues that are important for catalysis. In this investigation, pre-steady-state studies were performed on the His_6-tagged wild-type (WT) enzyme, several active site mutants, a thermostable mutant (12X-PTDH), and a thermostable mutant with dual cofactor specificity (NADP-12X-PTDH). Stopped-flow kinetic experiments indicate that slow steps after hydride transfer do not significantly limit the rate of reaction for the WT enzyme, the active site mutants, or the thermostable mutant. Pre-steady-state kinetic isotope effects (KIEs) and single-turnover experiments further confirm that slow steps after the chemical step do not significantly limit the rate of reaction for any of these proteins. Collectively, these results suggest that the hydride transfer step is fully rate determining in PTDH and that the observed KIE on k_{cat} is the intrinsic effect in WT PTDH and the mutants examined. In contrast, a slow step after catalysis may partially limit the rate of phosphite oxidation by NADP-12X-PTDH with NADP as the cofactor. Finally, site-directed mutagenesis of Asp79 indicates that this residue is important in orienting Arg237 for proper interaction with phosphite.

Phosphite dehydrogenase (PTDH)[1] is a unique NAD-dependent enzyme that was first isolated from *Pseudomonas stutzeri* WW88 (*1*, *2*). PTDH catalyzes the oxidation of inorganic phosphite to phosphate (Scheme 1), allowing the organism to use phosphite as its sole phosphorus source. The reaction represents an intriguing phosphoryl transfer reaction in which water or hydroxide is the phosphoryl acceptor. The enzyme has been shown to have great potential for cofactor regeneration (*3*), and its substrate specificity has been expanded to include the commercially important cofactor NADP (*4*). Subsequent directed evolution led to a mutant enzyme with increased activity (*5*) and substantially improved thermostability (*6*), thus enhancing the industrial utility of the enzyme.

In addition to the engineering work, several studies have probed the mechanistic details of the unusual enzymatic transformation catalyzed by PTDH (*7*−*11*). Although the reaction resembles a phosphoryl transfer process, the enzyme shows significant sequence homology (26−35%) to the D-hydroxy acid dehydrogenase family of enzymes (*2*). Using this homology, important active site residues have been identified in PTDH, and site-directed mutagenesis studies have investigated the roles they play in catalysis. Arg237 and Glu266 were shown to be important substrate binding residues, whereas His292 mutants demonstrated that this residue is critical for catalysis in PTDH and may act as the active site base to activate the water nucleophile (*7*). A recently solved X-ray crystallographic structure of the thermostable 12X-PTDH mutant (S. Nair, unpublished results) confirmed the presence of these residues in the active site and provided further support for the roles they play in catalysis (Figure 1). In addition, the X-ray crystallographic structure suggests additional roles for other residues. For example, Asp79 is involved in a hydrogen bond/ionic interaction with Arg237 and possibly acts to orient Arg237 such that it properly positions the substrate phosphite for hydride transfer. Kinetic isotope effect (KIE) studies with deuterium-labeled phosphite demonstrated significant isotope effects on V_{max} (^{D}V) and $V_{max}/K_{m,Pt}$ [$^{D}(V/K)$], indicating hydride transfer is at least partially rate determining for the enzyme (*8*, *10*). This finding is somewhat surprising considering the very favorable energetics of the reaction at pH 7.0, which strongly favors oxidation of phosphite to form phosphate ($E^{0\prime} = -0.648$ V) while reducing NAD^+ to NADH ($E^{0\prime} = -0.320$ V). This leads to an essentially irreversible

Scheme 1

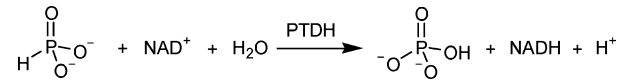

* To whom correspondence should be addressed. Phone: (217) 244-5360. Fax: (217) 244-8068. E-mail: vddonk@uiuc.edu.

† This work was supported by the National Institutes of Health (Grant GM63003).

[1] Abbreviations: PTDH, phosphite dehydrogenase; NAD, β-nicotinamide adenine dinucleotide; WT, wild type; 12X-PTDH, thermostable PTDH generated by random mutagenesis; NADP-12X-PTDH, NADP-specific 12X-PTDH; NADP, β-nicotinamide adenine dinucleotide phosphate; KIE, kinetic isotope effect; ^{D}V, primary kinetic isotope effect on V_{max}; $^{D}(V/K)$, primary kinetic isotope effect of $V/K_{m,Pt}$; LB, Luria−Bertani broth; OD_{600}, optical density at 600 nm; Tris, tris(hydroxymethyl)aminomethane; SDS−PAGE, sodium dodecyl sulfate−polyacrylamide gel electrophoresis; MOPS, 4-morpholinepropanesulfonic acid; PCR, polymerase chain reaction; UV−vis, ultraviolet−visible; ^{1}H-phosphite, protiated phosphite; ^{2}H-phosphite, deuterated phosphite; AU, absorbance unit; $^{D}k_{obsd}$, primary kinetic isotope effect observed in the pre steady state; C_f, commitment to catalysis; R_f, ratio of catalysis; E_f, equilibrium preceding catalysis; ^{D}k, intrinsic isotope effect.

10.1021/bi701550c CCC: $37.00
Published on Web 10/20/2007

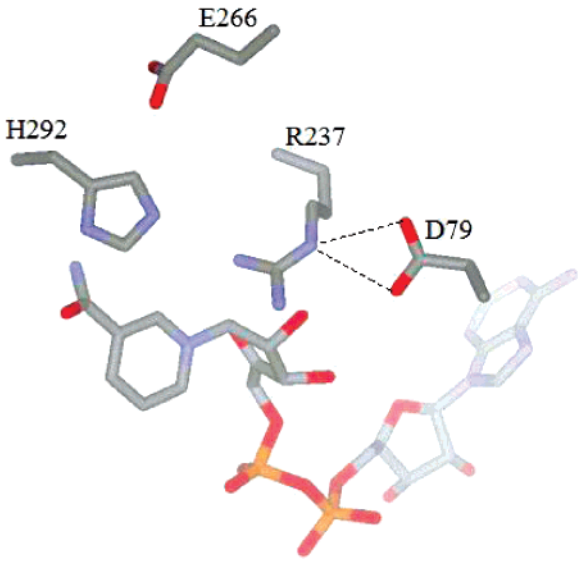

FIGURE 1: Active site structure of 12X-PTDH.

reaction with an equilibrium constant of 10^{11}. Given the favorable thermodynamics for the reaction, it is tempting to envision an enzyme with a rapid chemical step limited by slow physical steps, such as product release or a slow conformational change. To evaluate the degree to which the hydride transfer is rate limiting in PTDH, pre-steady-state studies were performed on the WT enzyme, several active site mutants, the thermostable 12X-PTDH mutant, and the thermostable mutant NADP-12X-PTDH that has relaxed cofactor specificity and can utilize both NAD and NADP. These studies indicate that slow steps after hydride transfer do not limit the rate of reaction for wild-type PTDH and its mutants. Collectively, the results suggest that the hydride transfer step is fully rate determining for k_{cat} and that the observed KIE is the intrinsic effect in the WT and the mutants examined. A smaller isotope effect observed with k_{cat}/K_m compared to k_{cat} suggests that substrate dissociation is somewhat slower than hydride transfer under conditions of low substrate concentration.

MATERIALS AND METHODS

Materials. Sodium phosphite was purchased from Fluka. All other chemicals were purchased from either Sigma or Aldrich unless otherwise noted.

Overexpression and Purification of WT and Mutant PTDH. His_6-tagged PTDH was overexpressed as reported previously (*10*). The His tag was shown in a prior study not to have a significant effect on the kinetics of the enzyme (*4*). Briefly, 3 L of LB was inoculated with ~20 mL of an overnight culture of *Escherichia coli* BL21(DE3) harboring a pET15b vector containing the PTDH gene and grown at 37 °C until $OD_{600} = 0.4$. The culture was cooled on ice for ~20 min, and IPTG was added to a concentration of 0.3 mM. The culture was grown at 25 °C for 8−10 h following induction. The cells were pelleted by centrifugation (5000*g*, 20 min), resuspended in 20 mM Tris, pH 7.6, 500 mM NaCl, and 10% (v/v) glycerol, and stored at −80 °C. The resuspended cell pellet was thawed on ice, incubated with 0.3 mg/mL lysozyme for 20 min, and then sonicated for 15 min with a pulse sequence of 5 s on, 9.9 s off. After removal of cell debris by centrifugation (15000*g*, 30 min), the cell-free extract was filtered (0.44 μm) and loaded onto an 8 mL POROS (PerSeptive Biosystems) metal chelate affinity column loaded with Ni^{2+} and equilibrated in buffer A. The column was washed with 10−20 column volumes of buffer A followed by a linear gradient of 20 column volumes from 100% buffer A to 100% buffer B (buffer A, 20 mM Tris, pH 7.6, 100 mM NaCl, 10 mM imidazole, 10% (v/v) glycerol; buffer B, 20 mM Tris, pH 7.6, 100 mM NaCl, 500 mM imidazole, 10% (v/ v) glycerol). The fractions containing PTDH, as determined by absorbance at 280 nm, SDS−PAGE, and enzyme activity, were pooled, concentrated, dialyzed into 50 mM MOPS, pH 7.25, and flash frozen. The protein concentration was determined using a calculated extinction coefficient for PTDH, 28 000 M^{-1} cm^{-1}.

Preparation of D79A PTDH. The mutant was made using the Quik Change protocol (Stratagene) with some modifications. The primer pair used to introduce the desired mutation was D79A: 5′-GCG CTC AAG GGC TTC GCA AAT TTC GAT GTG GAC GCC-3′ and 5′-GGC GTC CAC ATC GAA ATT TGC GAA GCC CTT GAG CGC-3′ (with the mutated codon underlined). The primers were desalted, and the PCR reaction used Pfx polymerase. Once the mutant genes were constructed, they were sequenced in their entirety to ensure that the desired mutation was incorporated and no other mutations were generated.

Steady-State Kinetic Assays. Initial rates were obtained at 25 °C using a Cary 100 Bio UV−vis spectrophotometer (Varian). The concentrations of stock NAD solutions were determined using the extinction coefficient (NAD, $\epsilon_{260} =$ 18 000 M^{-1} cm^{-1}) (*12*). The concentrations of phosphite stock solutions were determined by adding PTDH and excess NAD, incubating the reaction at 25 °C until complete, and determining the concentration of NADH produced using its extinction coefficient. Reactions were monitored by the formation of NADH by absorbance at 340 nm. Typical reactions were performed in 100 mM MOPS, pH 7.25, with 0.2−0.5 μM PTDH, and varying concentrations of NAD and phosphite.

Steady-State Kinetic Isotope Effects. KIEs were determined by holding the NAD concentration at $10K_m$ and varying the concentration of either ^{1}H- or ^{2}H-phosphite. It has been shown previously that PTDH observes an ordered mechanism in which NAD binds first (*2*), resulting in no observed KIE on $V/K_{m,NAD}$ (*10*). The data in this study were fitted to the Michaelis−Menten equation to obtain V_{max} and $K_{m,Pt}$. Direct comparison of the kinetic parameters determined with ^{1}H- and ^{2}H-phosphite gave ^DV and $^D(V/K_{m,Pt})$.

Pre-Steady-State Kinetics and KIEs of the WT and Active Site Mutants. Pre-steady-state kinetic experiments were performed using an Olis RSM 1000 stopped flow spectrophotometer. The dead time of the instrument under experimental conditions was determined to be ~4 ms using ascorbate and 2,6-dichloroindophenol (*13*). Data were collected between 320 and 420 nm at a rate of 1000 scans/s for a total time of 1−2 s for traces with the WT and all mutants except R237K and D79A. For the latter, less active mutants data were collected in the same wavelength range but at a rate of 62 scans/s for a total time of 30 s. For all experiments, one syringe contained PTDH in 100 mM MOPS, pH 7.25, and the other syringe contained NAD and either ^{1}H- or ^{2}H-phosphite such that the final concentration of both substrates was saturating ($\sim 10K_m$) after mixing, also in 100 mM

Table 1: Steady-State Kinetic Constants for Asp79 and Arg237 Mutants[a]

	k_{cat} (s^{-1})	$K_{m,Pt}$ (μM)	$K_{m,NAD}$ (μM)	$k_{cat}/K_{m,Pt}$ ($M^{-1}\,s^{-1}$)
WT	2.42(0.03)	55(5)	35(5)	6.5(0.7) × 10^4
D79A	0.0305(0.0008)	1200(100)	62(3)	25(2)
D79N	0.23(0.01)	35(5)	12(1)	6.60(0.90) × 10^3
R237K	0.0126(0.0006)	1.00(0.10) × 10^4	1000(100)	1.25(0.14)

[a] All assays were performed at 25 °C, pH 7.25, in 100 mM MOPS. The steady-state parameters k_{cat} and $K_{m,Pt}$ were measured at saturating concentrations of NAD, and the phosphite concentration was varied; $K_{m,NAD}$ was determined by holding the phosphite concentration at a saturating level and varying the concentration of NAD. The errors given in parentheses were obtained from fitting to the Michaelis−Menten equation.

MOPS, pH 7.25. The final concentration of enzyme was 15 μM for the WT and all of the mutants tested, except R237K and D79A, for which the final concentrations were 33 and 28 μM, respectively. Aggregation and precipitation of the enzymes did not allow the use of higher concentrations of enzyme. The traces shown here are the average of four shots. k_{obsd} was calculated by fitting the data to a zeroth-order equation; the errors given for k_{obsd} are the standard deviation of four individual shots. Controls showed that none of the $t = 0$ absorbance is due to product formation within the dead time of the stopped flow instrument.

Pre-Steady-State Kinetics and KIEs of Thermostable 12X-PTDH and NADP-12X-PTDH. Pre-steady-state kinetic studies were performed as described above except higher concentrations of enzyme could be used because of the higher solubility of these proteins. For 12X-PTDH, the final concentration of enzyme was 150 μM and the concentrations of all substrates were 5 mM. The data were fit to a zeroth-order equation as described above. The traces are the average of four shots. For NADP-12X-PTDH, the final concentration of enzyme was 120 μM and the concentration of all substrates was 2.5 mM. When NAD was used, the traces were fit to a zeroth-order equation. The curvature in the traces when NADP was used as a substrate prevented fitting to a zeroth-order equation. The data were not well fit by the burst equation (eq 1) (*14*).

$$dP/dt = A(1 - e^{k_b t}) + k_{cat} t \quad (1)$$

Single-Turnover Experiments with 12X-PTDH. For single-turnover experiments data were collected between 320 and 420 nm at a rate of 1000 scans/s for a total time of 2 s for ^{1}H-phosphite and at a rate of 62 scans/s for a total time of 4 s for ^{2}H-phosphite. These experiments used 2.5 mM NAD, 150 μM ^{1}H- or ^{2}H-phosphite, and 150 μM 12X-PTDH PTDH. The data were fit to a single-exponential equation.

RESULTS

Steady-State Kinetics of Asp79 Mutants. The D79A mutant showed significant differences in its kinetic constants compared to the WT enzyme (Table 1). Whereas $K_{m,NAD}$ remained relatively unaffected, the value of k_{cat} decreased approximately 80-fold and $K_{m,Pt}$ increased about 20-fold, leading to a 2600-fold decrease in catalytic efficiency. On the other hand, the D79N mutant had kinetic parameters more similar to those of WT. The mutant displayed only a 10-fold decrease in k_{cat}, whereas the K_m values for phosphite and NAD were essentially unaffected (Table 1).

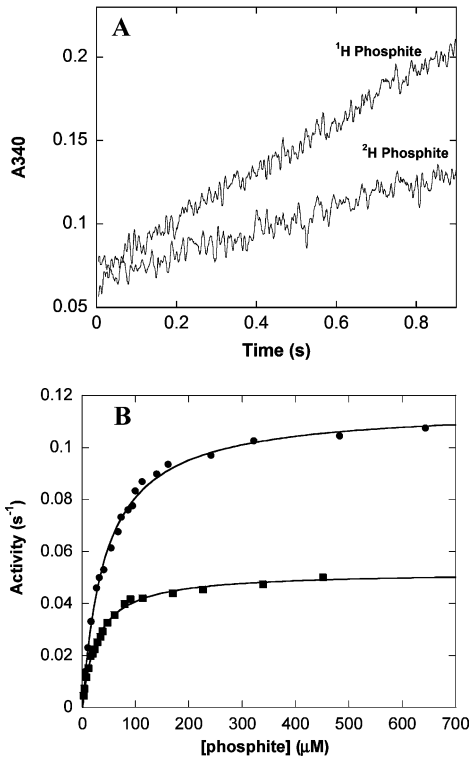

FIGURE 2: Reaction of wild-type PTDH with protiated and deuterated phosphite in the steady state and pre steady state. (A) Average of four pre-steady-state traces in which a solution of 15 μM WT PTDH was mixed with an equal volume of a solution of 500 μM ^{1}H- or ^{2}H-phosphite and 500 μM NAD^+ in 50 mM MOPS, pH 7.25. (B) Phosphite concentration dependence of the steady-state activity of 0.13 μM PTDH in the presence of 1 mM NAD^+ in 100 mM MOPS, pH 7.25. The lines represent fits to the Michaelis−Menten equation for protiated (circles) and deuterated (squares) phosphite.

Pre-Steady-State Kinetics of WT PTDH. The pre-steady-state behavior of PTDH was investigated to determine whether step(s) after catalysis were partially rate determining. WT PTDH showed no clear pre-steady-state burst of activity (Figure 2A). The trace does not show any obvious curvature, and at time $t = 0$ the absorbance is ~0.05 absorbance unit (AU) when uncorrected for the absorbance of the enzyme and substrates; when corrected, the $t = 0$ absorbance is approximately 0. The amplitude of a full stoichiometric burst would be expected to be ~0.1 AU on the basis of the amount of enzyme used in the experiment, suggesting that a stoichiometric burst does not take place in the dead time of the instrument. Because it was not possible to increase the enzyme concentration to enhance any burst amplitude due to aggregation and precipitation of the enzyme, we cannot definitely rule out the possibility that a small substoichiometric burst occurs within the dead time of the instrument. The similarity of the pre-steady-state and steady-state rates provides additional support that no rapid reaction occurs upon the initial mixing of the enzyme and substrates.

Pre-Steady-State KIEs with WT PTDH. Comparison of the rates in the pre steady state using ^{1}H- and ^{2}H-phosphite allows determination of the observed isotope effect in the pre steady state, $^D k_{obsd}$ (Figure 2A and Table 2). The primary substrate KIE in the pre steady state was determined to be

Table 2: Steady-State Kinetic Parameters for NADP-12X-PTDH[a]

	k_{cat} (s^{-1})	$k_{cat}/K_{m,Pt}$ ($M^{-1}s^{-1}$)	^{D}V	$^{D}(V/K)$
12X	3.26(0.15)	$7.6(1.1) \times 10^4$	2.5(0.15)	1.0(0.2)
NADP-12X NAD	2.04(0.04)	$4.3(0.2) \times 10^4$	2.17(0.08)	1.48(0.18)
NADP-12X NADP	0.58(0.02)	$2.5(0.3) \times 10^4$	1.66(0.07)	1.1(0.2)

[a] All assays were performed at 25 °C, pH 7.25, in 100 mM MOPS. The steady-state parameters k_{cat} and $K_{m,Pt}$ were measured at saturating concentrations of NAD or NADP, and the phosphite concentration was varied. The errors given in parentheses are obtained from fitting to the Michaelis−Menten equation.

$^{D}k_{obsd} = 2.0(0.2)$ (Table 2), in good agreement with the steady-state KIE on V_{max}, $^{D}V = 2.22(0.03)$ (Figure 2B).

Pre-Steady-State Kinetics of 12X-PTDH. The pre-steady-state behavior of the thermostable mutant 12X-PTDH was investigated next because of its current use in commercial settings. This enzyme does not aggregate at high enzyme concentrations, allowing pre-steady-state studies that used ~10-fold more enzyme than the experiments with WT PTDH. Pre-steady-state traces did not show a burst of activity nor any curvature during the period of data collection (Figure 3A). A stoichiometric burst within the dead time of the stopped flow instrument can be definitively ruled out; on the basis of the amount of enzyme used, the burst amplitude would have been ~0.9 AU. It is clear from the trace that no such burst occurs within the dead time of the stopped flow instrument. A significant substoichiometric burst can also be ruled out for 12X-PTDH; if the burst amplitude were reduced by 90%, the expected burst would be ~0.09 AU. Clearly, such a burst does not occur within the dead time of the instrument or during the course of the experiment. In addition, the rate observed in the pre steady state is within error of the steady-state k_{cat} (Table 2). Collectively, these observations indicate that a step after catalysis is not partially rate limiting for 12X-PTDH. As found for WT PTDH, the isotope effect for 12X-PTDH observed in the pre steady state, $^{D}k_{obsd} = 2.23(0.15)$, is in good agreement with the observed isotope effect on V_{max} ($^{D}V = 2.50(0.15)$, Table 2).

Single-Turnover Experiments with 12X-PTDH. The higher solubility of 12X-PTDH allowed investigation of the pre-steady-state behavior under single-turnover conditions using 150 μM enzyme. These single-turnover experiments were performed to probe whether a step involving phosphite binding or a conformational change associated with binding could be partially rate limiting. At phosphite concentrations of 50−150 μM, the experimental traces for ^{1}H- and ^{2}H-phosphite were well fit by a single-exponential equation without any evidence for a lag phase (Figure 3B). The observed rates under single-turnover conditions for ^{1}H-phosphite were similar to the steady-state rates under the same conditions, providing further evidence that steps after hydride transfer are not rate determining. Unfortunately, attempts to separate binding steps from catalysis in these experiments were unsuccessful. The observed rates were independent of phosphite concentrations under conditions that still provided reliable absorbance changes (30−150 μM), suggesting that $K_{D,Pt}$ is below 25 μM. The isotope effect under single-turnover conditions was determined to be 2.2-(0.16), close to the isotope effect observed in the pre-steady-state multiple-turnover studies determined under saturating concentrations of substrates, $^{D}k_{obsd} = 2.23(0.15)$. Furthermore, the isotope effect determined under single-turnover conditions was not significantly reduced compared to the steady-state effect, $^{D}V = 2.5(0.15)$.

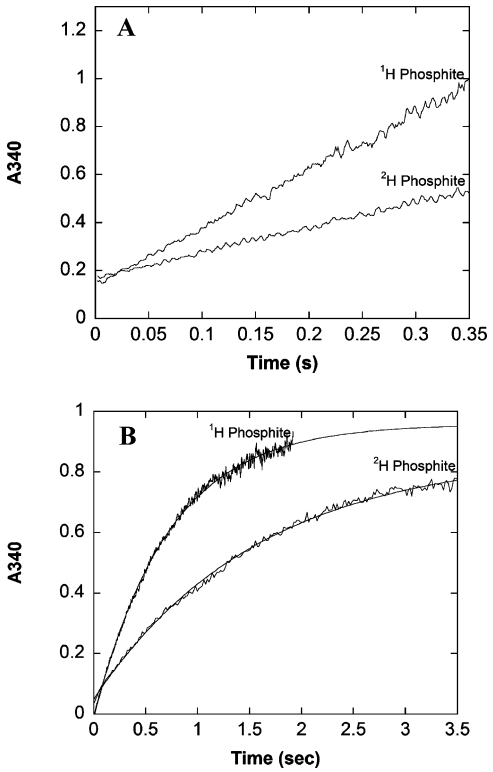

FIGURE 3: Pre-steady-state traces for 12X-PTDH. (A) Traces with saturating NAD^+ and ^{1}H- or ^{2}H-phosphite. Reaction conditions: 100 mM MOPS, pH 7.25, 5 mM ^{1}H- or ^{2}H-phosphite, 5 mM NAD, 150 μM 12X-PTDH. Each trace is the average of four separate shots. (B) Single-turnover experiments with ^{1}H- or ^{2}H-phosphite. Reaction conditions: 100 mM MOPS, pH 7.25, 150 μM ^{1}H- or ^{2}H-phosphite, 2.5 mM NAD^+, 150 μM 12X-PTDH. Each trace is the average of four separate shots. The solid line represents the fit to a single-exponential equation.

Steady-State KIEs of NADP-12X-PTDH. Steady-state KIEs were determined next for the engineered PTDH mutant with dual-cofactor specificity using both NAD and NADP as substrates (Table 3). With NAD as a substrate ^{D}V was 2.17-(0.08), but when NADP was used, this value decreased significantly to 1.66(0.07). This same trend was also observed previously with the dual-cofactor specificity mutant in the WT background (i.e., without the mutations conferring the increased thermostability) (*15*). The k_{cat} value with NADP as a substrate also decreased ~6-fold compared to when NAD was used as the cofactor (Table 3).

Pre-Steady-State Behavior of NADP-12X-PTDH with NAD as the Substrate. The pre-steady-state behavior of NADP-12X-PTDH with NAD (Figure 4A) is very similar to that observed with 12X-PTDH and the wild-type enzyme. The trace is linear, no significant burst of activity in the pre steady state is observed, and the rate in the pre steady state, $k_{obsd} = 2.1(0.2)\ s^{-1}$, is within error of the steady-state rate, $k_{cat} = 2.04(0.04)\ s^{-1}$. The isotope effect observed in the pre steady state, $^{D}k_{obsd} = 2.26(0.23)$, is also within error of $^{D}V = 2.17-(0.08)$, as observed with the other enzymes tested.

Pre-Steady-State Behavior of NADP-12X-PTDH with NADP as the Substrate. The pre-steady-state kinetics of NADP-12X-PTDH with NADP as the cofactor were investigated to evaluate the possibility that a step after catalysis

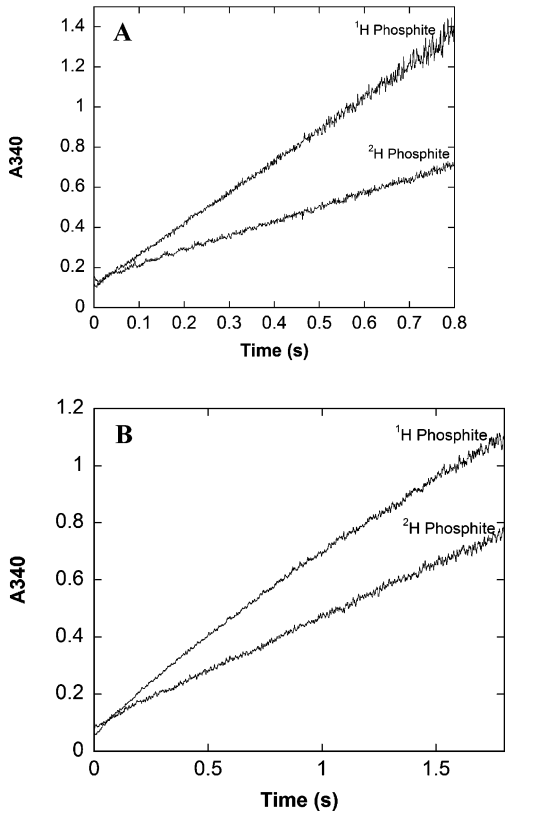

FIGURE 4: Pre-steady-state traces for NADP-12X-PTDH. (A) Traces with saturating NAD^+ and ^{1}H- or ^{2}H-phosphite. Reaction conditions: 100 mM MOPS, pH 7.25, 5 mM ^{1}H- or ^{2}H-phosphite, 5 mM NAD^+, 123 μM NADP-12X-PTDH. Each trace is the average of four separate shots. (B) Traces with saturating NADP and ^{1}H- or ^{2}H-phosphite. Reaction conditions: 100 mM MOPS, pH 7.25, 5 mM ^{1}H- or ^{2}H-phosphite, 5 mM NADP, 123 μM NADP-12X-PTDH. Each trace is the average of four separate shots.

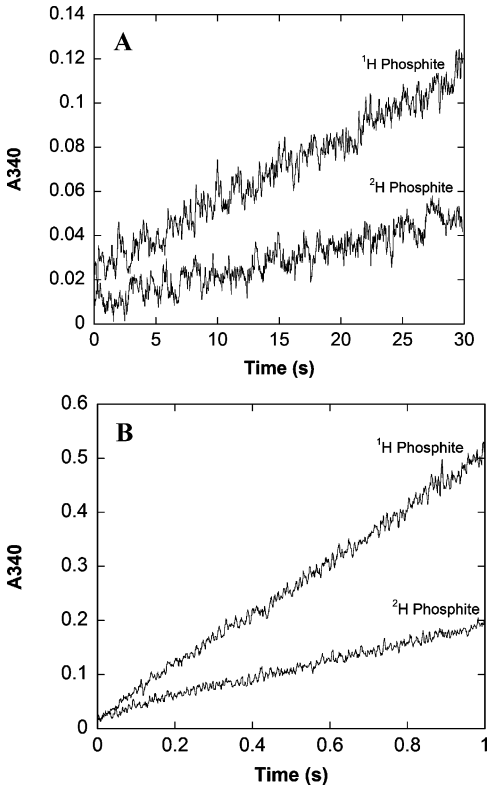

FIGURE 5: Reaction of representative active site mutants with protiated and deuterated phosphite in the pre steady state. (A) Reaction of R237K with protiated and deuterated phosphite in the pre steady state. Reaction conditions: 100 mM MOPS, pH 7.25, 100 mM ^{1}H- or ^{2}H-phosphite, 10 mM NAD^+, 33 μM R237K. (B) Reaction of E266Q with protiated and deuterated phosphite in the pre steady state. Reaction conditions: 100 mM MOPS, pH 7.25, 100 mM ^{1}H- or ^{2}H-phosphite, 5 mM NAD^+, 15 μM E266Q. Each trace is the average of four separate shots. The background due to absorbance of NAD^+ at 340 nm has been subtracted.

becomes partially rate determining, providing a possible explanation for the observed decreases in k_{cat} and ^DV in the steady-state experiments discussed above (Table 3). In contrast to what was observed when NAD was used as the cofactor, the pre-steady-state traces showed curvature with NADP, particularly with protiated phosphite (Figure 4B). The curvature is not due to consumption of substrates; only ~3% of the substrates were consumed during the period of data collection. The curvature is most likely due to burst kinetics in the pre steady state. Analysis of the data finds that the rate immediately after mixing of the enzyme and substrates is ~2-fold larger than k_{cat} and then decreases to nearly k_{cat} at the latest time points collected. We were unable to accurately fit the data to the generic burst equation (*14*).

Pre-Steady-State Kinetics of PTDH Active Site Mutants. The pre-steady-state behavior of the active site mutants K76A, R237K, E266Q, and D79A was investigated as they have steady-state rates spanning more than 3 orders of magnitude. Pre-steady-state traces for R237K and E266Q are shown in Figure 5. The trace for R237K has a relatively low signal-to-noise ratio because the low activity of the mutant leads to a relatively small absorbance change. As for the WT enzyme, aggregation of the protein occurs at higher concentrations for all of the mutants tested, precluding studies using higher enzyme concentrations that would generate a larger absorbance change and improve the signal-to-noise ratio. Although noisy, the R237K trace (Figure 5A) shows the absence of a significant burst in the pre steady state for this mutant. The data shown in Figure 5 correspond to less than 1 half-life, but the observed rate (1.52×10^{-2} s^{-1}) is in very good agreement with the steady-state rate for this mutant under saturating conditions (1.26×10^{-2} s^{-1}), again indicating that no significant burst occurs. Similarly, no observable burst of activity was observed in the pre steady state for K76A or D79A (data not shown), and their pre-steady-state rates are approximately the same as the steady-state rates (Table 2). The signal-to-noise ratio is much improved for E266Q, which has higher activity, but for this mutant as well a significant burst of product formation was not observed in the first 2 half-lives, and the steady-state and pre-steady-state rates are comparable (Figure 5B). The lack of a clear burst in the pre steady state suggests a step after catalysis does not significantly limit the rate of reaction for all of the active site mutants tested.

For completeness, the isotope effects in the pre steady state were also determined for these mutants. As expected on the basis of the lack of burst kinetics, the isotope effect in the pre steady state for R237K, $^Dk_{obsd} = 2.37(0.35)$, was within error of $^DV = 2.36(0.06)$, whereas for E266Q $^Dk_{obsd}$ was 3.3-(0.3), also within error of the steady-state KIE, $^DV = 3.3$-(0.1). In fact, $^Dk_{obsd}$ was within error of the steady-state ^DV for all of the mutants tested (Table 2).

Table 3: Summary of Steady-State and Pre-Steady-State Kinetic Constants for WT PTDH and Mutants[a]

	steady state[b]				pre steady state[c]	
	k_{cat} (s^{-1})	$k_{cat}/K_{m,Pt}$ ($M^{-1}\,s^{-1}$)	$^{D}(V/K_{m,Pt})$	^{D}V	k_{obsd} (s^{-1})	$^{D}k_{obsd}$
WT	2.42(0.03)	$6.5(0.7) \times 10^4$	1.44(0.08)	2.22(0.03)	1.56(0.02)	2.0(0.1)
E266Q	7.5(0.1)	250(10)	1.78(0.15)	3.3 (0.1)	5.3(0.5)	3.0(0.3)
K76A	0.62(0.01)	295(15)	1.9(0.1)	2.34(0.04)	0.42(0.07)	2.1(0.4)
R237K	0.0126(0.0006)	1.25(0.14)	2.1(0.3)	2.36(0.06)	0.0152(0.002)	2.37(0.35)
D79A	0.0305(0.0008)	25(2)	1.5(0.1)	1.97(0.08)	0.0188(0.0007)	2.01(0.16)
12X-PTDH	3.25(0.15)	$7.6(1.1) \times 10^4$	1.0(0.2)	2.50(0.15)	2.5(0.1)	2.23(0.15)

[a] All assays were performed at 25 °C and pH 7.25 in 100 mM MOPS. [b] The steady-state parameters were measured at saturating NAD concentration for each enzyme tested, and the phosphite concentration was varied. The errors given in parentheses were obtained from fitting to the Michaelis−Menten equation. [c] The pre-steady-state studies were performed at saturating phosphite and NAD concentrations for each mutant studied. k_{obsd} was obtained by fitting the absorbance change observed in the pre steady state to a zeroth-order equation; the errors given in parentheses are standard deviations.

DISCUSSION

The reaction catalyzed by PTDH, the oxidation of inorganic phosphite to phosphate (Scheme 1), represents an intriguing phosphoryl transfer reaction in which water or hydroxide is the phosphoryl acceptor. Previous site-directed mutagenesis studies (*7*) have investigated the roles played by several active site residues in catalysis. These studies demonstrated the importance of Arg237 and Glu266 for phosphite binding and the critical importance of His292 for catalysis. The recently solved X-ray crystallographic structure (unpublished data) has confirmed the presence of these residues in the enzyme active site and has suggested other residues that might be important to enzyme function (Figure 1). In the structure, the conserved Asp79 interacts with Arg237, but is not expected to make direct contacts with phosphite. The site-directed mutagenesis studies presented here suggest that Asp79 acts to orient Arg237. The D79A mutation, which eliminates any functionality that could hold Arg237 in place, led to significantly decreased values of both k_{cat} and $k_{cat}/K_{m,Pt}$ and a large increase in $K_{m,Pt}$ compared to the WT enzyme (Table 1). In fact, the kinetic constants for D79A are similar to those found for R237K, a mutant in which the arginine that directly interacts with phosphite is mutated to lysine. In contrast, the D79N mutant has nearly WT activity, and $K_{m,Pt}$ has actually decreased compared to that of the WT (Table 1). Presumably the hydrogen-bonding interactions between Asn79 and Arg237 are sufficient to position the arginine for efficient binding of phosphite.

The extremely favorable energetics of the reaction catalyzed by PTDH, $K_{eq} = 10^{11}$, make it tempting to envision a mechanism in which the chemical step of hydride transfer is rapid and the steady-state rate is determined by physical steps such as product release or a slow conformational change. However, previous studies with PTDH showed significant KIEs on both V_{max} and $V/K_{m,Pt}$, indicating that the chemical step of hydride transfer is at least partially rate determining (*8*). The isotope effect on $V/K_{m,NAD}$ was unity, consistent with an ordered mechanism with NAD binding first. It should be noted that the values found for the isotope effects are larger than they may first appear because the theoretical maximal classical isotope effect has been calculated to be 5.0 at 25 °C on the basis of infrared stretching frequencies of P−H and P−D bonds (*10*). Unlike other dehydrogenases (*16*), the possibility of quantum mechanical tunneling has not yet been investigated for PTDH.

When KIEs were determined for active site mutants such as K76A and R237K, the isotope effect observed on V_{max} was within error of the effect on the WT. Considering that the catalytic efficiency of these mutants is diminished by up to 4 orders of magnitude compared to that of the WT enzyme and that k_{cat} is decreased by more than 100-fold, identical V_{max} isotope effects in the mutants and WT present the possibility that the observed isotope effect may be the intrinsic effect; i.e., the observed KIE on V_{max} is not masked by other steps. To evaluate the degree to which the hydride transfer step is rate limiting in PTDH, pre-steady-state studies were performed on the WT enzyme, several active site mutants, and the thermostable 12X-PTDH mutant. Studies with the WT enzyme did not show a significant burst of activity nor clear curvature during the course of the measurement or in the dead time of the stopped flow instrument. The same behavior was observed for several active site mutants including E266Q, K76A, R237K, and D79A and the thermostable mutants 12X-PTDH and NADP-12X-PTDH with NAD as a substrate. These results indicate that slow steps after hydride transfer, such as product release or a slow conformational change, do not significantly limit the steady-state rate in the WT enzyme and mutants tested. Attempts to confirm this conclusion by determining both the deuterium and tritium KIEs using the method of Northrop (*17*) were inconclusive due to the relatively large error in the tritium isotope effects. Single-turnover experiments with the 12X-PTDH mutant also did not provide any evidence that steps preceding catalysis limit the rate of reaction for 12X-PTDH.

The pre-steady-state behavior of NADP-12X-PTDH using the alternate cofactor NADP differs from that observed with the WT and other PTDH mutants. The rate immediately after mixing the enzyme and substrates is ~2-fold faster than the steady-state rate, suggesting that a step after catalysis is partially rate determining for this mutant under these conditions. This model is consistent with the decrease in both k_{cat} and the steady-state KIE in this mutant when NADP is used as the cofactor (Table 2). Together with the small dissociation constant previously determined for NADPH for the NADP-specific mutations in the WT background (*15*), the data suggest that product release may be partially rate determining for NADP-12X-PTDH using NADP as a cofactor.

In several other enzymes where chemistry has been shown to be fully rate limiting (*18*−*20*) it was observed that the isotope effects on V_{max} and V/K were the same as the result of a very small or no commitment to catalysis. In PTDH ^{D}V is greater than $^{D}(V/K)$ for the WT and all the active site mutants tested (Table 2). This finding suggests that PTDH

Scheme 2

$$EA + B \underset{k_4}{\overset{k_3}{\rightleftharpoons}} EAB \xrightarrow{k_5} EPQ \xrightarrow{k_7} E + P + Q$$

may have a relatively large forward commitment to catalysis. Examination of the expressions for ^{D}V (eq 2) and $^{D}(V/K)$ (eq 3),

$$^{D}(V/K) = \frac{^{D}k + C_f}{1 + C_f} \quad (2)$$

$$^{D}V = \frac{^{D}k + R_f/E_f}{1 + R_f/E_f} \quad (3)$$

simplified for an irreversible reaction as occurs in PTDH, shows that ^{D}V and $^{D}(V/K)$ depend on different terms in addition to the intrinsic effect ^{D}k. Using Northrop's terminology (*21*), $^{D}(V/K)$ depends also on the commitment to catalysis, C_f, whereas ^{D}V depends on the ratio of R_f, the ratio of catalysis, to E_f, the equilibrium preceding catalysis (the ratio R_f/E_f has also been termed c_{Vf} in the nomenclature of Cleland (*22*)).

The terms C_f, R_f, and E_f in turn depend on different ratios of microscopic rate constants. The pre-steady-state data demonstrate that there are no kinetically important steps after catalysis, and the single-turnover experiments did not provide clear evidence for a slow conformational change prior to hydride transfer. Therefore, the minimal mechanism given in Scheme 2 can be used to represent the initial reaction rates catalyzed by PTDH in the presence of saturating concentrations of NAD. In this scheme, no equilibria precede catalysis under conditions of substrate saturation (^{D}V), and thus, E_f is unity. C_f and R_f are described by the expressions in eqs 4 and 5

$$C_f = \frac{k_5}{k_4} \quad (4)$$

$$R_f = \frac{k_5}{k_7} \quad (5)$$

(*21*). The stopped flow data clearly show that product release (k_7) must be much faster than hydride transfer (k_5), resulting in a value for R_f approaching 0 and observed isotope effects on V that are equal to the intrinsic KIE (eq 3). Phosphite release from the ternary complex (k_4) on the other hand cannot be much faster than the hydride transfer step to account for $^{D}(V/K)$ values that are smaller than those for ^{D}V. In the case of PTDH, the observed data are consistent with a rate of Michaelis complex dissociation (k_4) that is approximately 2-fold slower than the chemical step (k_5). In other words, the commitment to catalysis is about 2 as a result of a "sticky" substrate (*22*).

A free energy diagram describing the minimal kinetic mechanism is given in Figure 6A. The energy of the ES complex was determined from the K_d for phosphite calculated from $^{D}(V/K)$, ^{D}V, and $K_{m,Pt}$ using the method of Klinman and Matthews (*23*). The dissociation constant for phosphite so determined is 16 μM, which corresponds to an ES complex ~6.5 kcal/mol lower in energy than the NAD−enzyme complex and free phosphite. The total free energy

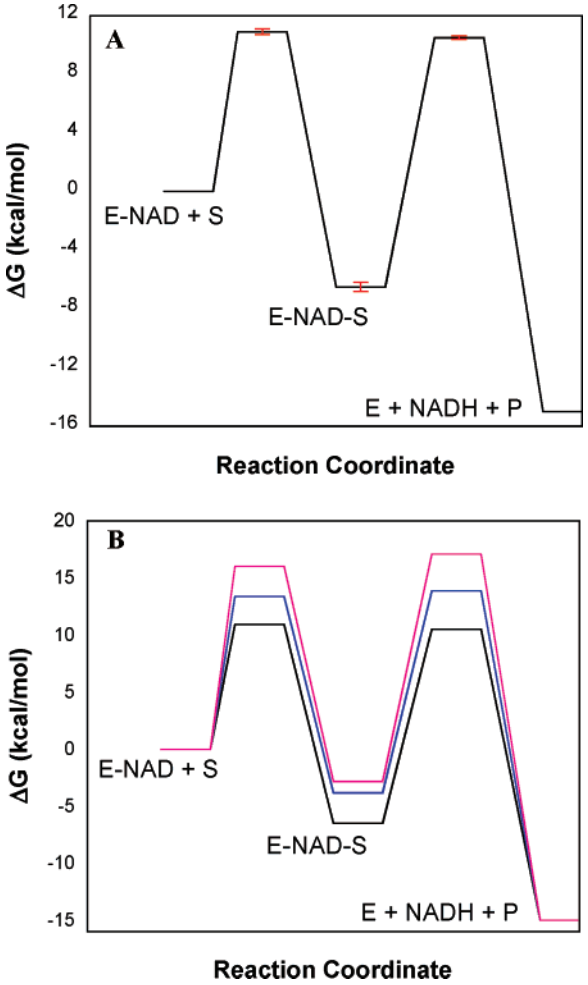

FIGURE 6: Proposed free energy diagram of the reaction catalyzed by PTDH (A) and PTDH mutants (B).

change for the reaction catalyzed by PTDH at pH 7.0 (15 kcal/mol) was determined from the redox potentials of phosphite and NAD as reported previously (*10*). As discussed above, the experimental data suggest that k_{cat} is fully limited by hydride transfer; thus, the barrier height for hydride transfer (17 kcal/mol) was calculated using the Eyring equation, assuming $k_5 = k_{cat}$. Using the experimentally determined isotope effect on V/K, the assumption of $k_5 = k_{cat}$, and the expression for $^{D}(V/K)$ given in eq 2, the value of k_4 and the barrier to the formation of the ES complex were determined. The free energy diagram depicted in Figure 6A accounts for the experimental observations of nearly identical V_{max} isotope effects in mutants with a wide range of catalytic efficiency and activity, a lack of a significant burst in the pre steady state, and identity between the steady-state ^{D}V and the isotope effects observed in the pre steady state. Such a kinetic mechanism predicts that as commitment to catalysis becomes smaller, i.e., the substrate becomes less sticky or k_5 becomes smaller than k_4, the isotope effect will become more fully expressed in $^{D}(V/K)$ to the limit where $^{D}(V/K) = {}^{D}V$. Interestingly, such a trend is observed in the active site mutants. Although $^{D}(V/K)$ never reaches the limit of ^{D}V, as k_{cat} decreases $^{D}(V/K)$ approaches ^{D}V in the active site mutants (Table 2). Free energy profiles for the K76A and R237K mutants, determined as described above for WT PTDH, show graphically the (small) decrease in commitment

to catalysis that occurs in these mutants compared to the WT (Figure 6B).

It has been noted that the classic picture of an enzyme-catalyzed reaction in which physical steps such as substrate binding and product release are rapid and a single chemical transformation step is slow and completely rate determining is often incorrect (*24*). More often enzymes have multiple rate determining steps, and in some cases the overall rate of reaction is not determined by chemistry at all and is entirely limited by physical steps (*25*). In fact, it has been suggested that during evolution the step with the largest barrier is being optimized, ultimately resulting in several partially rate determining steps (*26*). The observation that chemistry is fully rate determining in PTDH may suggest that the enzyme has only relatively recently evolved the ability to oxidize phosphite. However, the low sequence conservation between PTDH and another confirmed phosphite dehydrogenase (*27*) as well as putative phosphite dehydrogenases in the protein databases suggests that these enzymes may have had a long time to evolve and diverge. It is intriguing that the two members of the D-hydroxy acid dehydrogenase family catalyzing the thermodynamically most favorable reactions, formate dehydrogenase and phosphite dehydrogenase, are among the slowest enzymes in the family and that for both chemistry is fully rate limiting (*18*). The fact that we have not been able to improve the activity of PTDH significantly through in vitro evolution techniques (*5*) suggests that perhaps the nucleophilic displacement reaction catalyzed by PTDH has a relatively large intrinsic barrier.

REFERENCES

1. White, A. K., and Metcalf, W. W. (2004) The htx and ptx operons of Pseudomonas stutzeri WM88 are new members of the pho regulon, *J. Bacteriol. 186*, 5876−5882.
2. Costas, A. M., White, A. K., and Metcalf, W. W. (2001) Purification and characterization of a novel phosphorus-oxidizing enzyme from Pseudomonas stutzeri WM88, *J. Biol. Chem. 276*, 17429−17436.
3. Vrtis, J. M., White, A. K., Metcalf, W. W., and van der Donk, W. A. (2002) Phosphite dehydrogenase: a versatile cofactor-regeneration enzyme, *Angew. Chem., Int. Ed. 41*, 3257−3259.
4. Woodyer, R., van der Donk, W. A., and Zhao, H. (2003) Relaxing the nicotinamide cofactor specificity of phosphite dehydrogenase by rational design, *Biochemistry 42*, 11604−11614.
5. Woodyer, R., van der Donk, W. A., and Zhao, H. (2006) Optimizing a biocatalyst for improved NAD(P)H regeneration: directed evolution of phosphite dehydrogenase, *Comb. Chem. High Throughput Screening 9*, 237−245.
6. Johannes, T. W., Woodyer, R. D., and Zhao, H. (2005) Directed evolution of a thermostable phosphite dehydrogenase for NAD(P)H regeneration, *Appl. Environ. Microbiol. 71*, 5728−5734.
7. Woodyer, R., Wheatley, J. L., Relyea, H. A., Rimkus, S., and van der Donk, W. A. (2005) Site-directed mutagenesis of active site residues of phosphite dehydrogenase, *Biochemistry 44*, 4765−4774.
8. Relyea, H. A., Vrtis, J. M., Woodyer, R., Rimkus, S. A., and van der Donk, W. A. (2005) Inhibition and pH dependence of phosphite dehydrogenase, *Biochemistry 44*, 6640−6649.
9. Relyea, H. A., and van der Donk, W. A. (2005) Mechanism and applications of phosphite dehydrogenase, *Bioorg. Chem. 33*, 171−189.
10. Vrtis, J. M., White, A. K., Metcalf, W. W., and van der Donk, W. A. (2001) Phosphite dehydrogenase: an unusual phosphoryl transfer reaction, *J. Am. Chem. Soc. 123*, 2672−2673.
11. van der Donk, W. A., and Zhao, H. (2003) Recent developments in pyridine nucleotide regeneration, *Curr. Opin. Biotechnol. 14*, 421−426.
12. Trimboli, A. J., and Barber, M. J. (1994) Assimilatory nitrate reductase: reduction and inhibition by NADH/NAD+ analogs, *Arch. Biochem. Biophys. 315*, 48−53.
13. Hoa, G. H., and Douzou, P. (1973) Stopped flow method at subzero temperatures, *Anal. Biochem. 51*, 127−136.
14. Johnson, K. A. (1992) in *The Enzymes* (Sigman, D. S., Ed.) pp 1−61, Academic Press, San Diego.
15. Woodyer, R., Zhao, H., and van der Donk, W. A. (2005) Mechanistic investigation of a highly active phosphite dehydrogenase mutant and its application for NADPH regeneration, *FEBS J. 272*, 3816−3827.
16. Nagel, Z. D., and Klinman, J. P. (2006) Tunneling and dynamics in enzymatic hydride transfer, *Chem. Rev. 106*, 3095−3118.
17. Northrop, D. B. (1977) in *Isotope Effects on Enzyme-Catalyzed Reaction* (Cleland, W. W., O'Leary, M. H., and Northrop, D. B., Eds.) pp 122−152, University Park Press, Baltimore, MD.
18. Blanchard, J. S., and Cleland, W. W. (1980) Kinetic and chemical mechanisms of yeast formate dehydrogenase, *Biochemistry 19*, 3543−3550.
19. Patel, M. P., and Blanchard, J. S. (2001) Mycobacterium tuberculosis mycothione reductase: pH dependence of the kinetic parameters and kinetic isotope effects, *Biochemistry 40*, 5119−5126.
20. Sobrado, P., Daubner, S. C., and Fitzpatrick, P. F. (2001) Probing the relative timing of hydrogen abstraction steps in the flavocytochrome b2 reaction with primary and solvent deuterium isotope effects and mutant enzymes, *Biochemistry 40*, 994−1001.
21. Northrop, D. B. (1991) in *Enzyme Mechanism from Isotope Effects* (Cook, P. F., Ed.) pp 181−196, CRC Press, Boca Raton, FL.
22. Cook, P. F., and Cleland, W. W. (2007) *Enzyme Kinetics and Mechanism*, Garland Science, New York.
23. Klinman, J. P., and Matthews, R. G. (1985) Calculation of substrate dissociation constants from steady-state isotope effects in enzyme-catalyzed reactions, *J. Am. Chem. Soc. 107*, 1058−1060.
24. Northrop, D. B. (1975) Steady-state analysis of kinetic isotope effects in enzymic reactions, *Biochemistry 14*, 2644−2651.
25. Cleland, W. W., and Northrop, D. B. (1999) Energetics of substrate binding, catalysis, and product release, *Methods Enzymol. 308*, 3−27.
26. Burbaum, J. J., Raines, R. T., Albery, W. J., and Knowles, J. R. (1989) Evolutionary optimization of the catalytic effectiveness of an enzyme, *Biochemistry 28*, 9293−9305.
27. Wilson, M. M., and Metcalf, W. W. (2005) Genetic diversity and horizontal transfer of genes involved in the oxidation of reduced P compounds by Alcaligenes faecalis WM2072, *Appl. Environ. Microbiol. 71*, 290−296.

BI701550C